Study of Gamma-ray Shielding of Two Different Heavy Metals and their Combination for Cs-137 and Co-60 Sources

Mohamed E. M. Eisa
Department of Physics, Northern Border University, Saudi Arabia | Department of Physics, Sudan University of Science and Technology, Sudan
memeisa@yahoo.com
(corresponding author)

M. D. M. Ali
Department of Physics, Sudan University of Science and Technology, Sudan
mohameddaffallah@yahoo.com

Mustafa J. Abuualreish
Department of Chemistry, Northern Border University, Saudi Arabia
mustjeed_2008@hotmail.com

Received: 23 November 2022 | Revised: 7 December 2022 | Accepted: 12 December 2022

ABSTRACT

This article presents data collected by measurements of lead (Pb) and iron (Fe) and their combination as heavy shielding materials. Measurements were performed using gamma photon energies of 662, 1173, and 1332keV for the Cs-137 and Co-60 sources. The theoretical data part was calculated using WinXCom, Phy-X, and Py-MLUBF software packages. Tables and graphs of the photon Mass Attenuation Coefficient (MAC), Linear Attenuation Coefficient (LAC), Half Value Layer (HVL), Tenth Value Layer (TVL) and Mean Free Path (MFP) are presented for both heavy metals and their combination to study the shielding properties experimentally and theoretically. The results will contribute to the ongoing research as a database for future use.

Keywords-linear attenuation coefficient; photon mass attenuation coefficient; radiation resistance data; heavy metals; gamma photon energies; gamma radiation properties

I. INTRODUCTION

Radiation protective shields play many functions, the most important of which is to reduce radiation exposure [1]. Radioactivity is common in the rocks and soil, in the water and oceans, and even in our building and home materials [2-4]. With the increasing use of gamma radiation in various applications such as industry, medicine, agriculture, nuclear reactors, and particle accelerators, radiation exposure for longer duration can cause very harmful effects on human health. Therefore, the use of shielding becomes paramount [5]. The interaction with gamma radiation photons takes place in various processes like the photoelectric effect, incoherent scattering, coherent scattering, and pair production and depends upon the energy of the photons [6-7]. Possible exposure to radiation emitted from radionuclides can occur in houses, offices, and other working places. In order to be able to assess radiological hazard, it is important to study the levels of radiation emitted from these building materials [8]. Different radiation shielding materials have been developed in the past. Ionizing photons such as X-rays and gamma rays can change the chemical structures of molecules, which may result in biological damages, cellular level mutations, or deterioration of materials [9-10]. Protection of biological entities from the harmful effects of radiation exposure is a fundamental requirement in the application of nuclear technology. Radiation exposure can be avoided by methods involving time, distance, and shielding, with shielding being the most important method [11-14].

When a gamma-ray beam passes through a sample of thickness x (cm) under narrow beam geometry, the photons are transmitted according to Beer-Lambert's equation [2, 15, 16]:

$$I = I_0 e^{-\mu x} \quad (1)$$

where I_o and I represent the gamma-ray intensity before and after passing through the sample, respectively, and μ (cm^{-1}) is the Linear Attenuation Coefficient (LAC) of the sample.

The LAC can be described in terms of the Mass Attenuation Coefficient (MAC) as follows [10, 17-19]:

$$\mu = \left(\frac{\mu}{\rho}\right)\mu_s \quad (2)$$

where μ_s $\frac{\mu}{\rho}$ (cm^2 g^{-1}) is the MAC and ρ (g cm^{-3}) is the density of the sample.

The Mean Free Path (MFP) (cm) is:

$$MFP=\frac{1}{\mu} \quad (3)$$

The effectiveness of the shielding capability of a material to a photon can be described by the Half Value Layer (HVL) (cm) [20-21]:

$$HVL=\frac{ln(2)}{\mu} \quad (4)$$

Similarly, the Tenth Value Layer (TVL) (cm) is given by:

$$TVL=\frac{ln(10)}{\mu} \quad (5)$$

II. MATERIALS AND METHODS

Measurements were conducted at the irradiation room of the Secondary Standard Dosimetry Laboratory of the Sudan Atomic Energy Commission (SAEC) on model OB-85 gamma calibrator manufactured by the Buchler GmbH and by using Cs-137 and Co-60 radioactive sources. Experimental measurement Tables II-IV were constructed using a secondary standard ionization chamber which has a volume of 1000cm^3 and displays the radiation dose of the sources and the thicknesses. The ionization chamber was chosen to be the center of a sphere relative to the reference source in a 2m distance from the source to the reference point. The holder of shielding samples was placed close to the OB-85 gamma calibrator. The shielding materials were placed inside the holder one by one. This procedure was followed for all shielding materials [22, 23]. Through the measurements the intensity of radiation was recorded, before and after placing the shielding material in the holder. The experimental coefficients were evaluated using gamma energies of 662keV for Cs-137 and 1173 and 1332KeV for Co-60 and the gamma transmission parameters such as the MAC, HVL, MFP, and transmission factor were determined and calculated.

III. RESULTS

Density, chemical composition, and concentration of the iron and lead samples and their combination can be seen in Table I. Table II-III present the experimental results of the attenuation coefficients and HVLs of Fe and Pb slabs using different thicknesses and doses of Cs-137 and Co-60. Table IV presents the experimental results of the combination of Fe and PB using Cs-137 gamma ray. The theoretical coefficient of the two materials and their combination were determined using Py-MLUBF, Phy-X, and XCOM [24, 26, 28-31] software packages which gave very close results. The results were compared against the experimental findings and gave very good agreement. Tables V-VII present the simulation results of Fe and Pb shielding using Py-MLUBF [32-33], Phy-X and WinXCOM software. The combination of the two shielding materials, Pb and Fe, is shown in Tables VIII and IX. Figures 1 and 2 show the relation between HVL and MAC vs Energy by using Py-MLUBF for Fe. Figures 3 and 4 show the relation between HVL and MAC vs Energy by using Py-MLUBF for Fe and Pb calculated by Py-MLUBF for Cs-137. Figures 8 and 9 show the relation between the gamma ray shielding factor for Fe and Pb calculated by Py-MLUBF for energies of 1173 and 1333KeV, respectively for the Co-60 source [33].

TABLE I. DENSITY AND CHEMICAL CONCENTRATION OF LEAD (PB) AND IRON (FE) SAMPLES

Material		**Lead**	**Iron**
Density(g/cm^3)		11.34	7.87
Concentration(%)	Sn	0.0023	
	Sb	0.00051	
	Bi	0.0025	
	As	0.0019	
	Ag	0.00064	
	Cd	0.00006	
	Zn	0.00022	
	Te	0.00026	
	Au	0.00096	
	In	0.00015	
	Na	0.00028	
	Ca	0.001	
	Pb	99.99	0.006
	C		0.062
	Si		0.035
	Mn		0.345
	Cr		0
	Mo		0.022
	Ni	0.00029	0
	Al	0.00039	0.01
	Cu		0
	Ti		0
	V		0
	Nb		0
	Co		0.046
	W		0
	Fe		99.474

TABLE II. EXPERIMENTAL RESULTS FOR FE USING CS-137 AND CO-60

	Attenuation coefficients and HVL for Fe slabs using Cs-137 gamma rays with initial dose of 474.76µGy.				**Attenuation coefficients and HVL for Fe slabs using Co-60 gamma rays with initial dose of 1.906 µGy.**			
Thickness (cm)	**Dose (µGy)**	**LAC (cm^{-1})**	**MAC (cm^2/g)**	**HVL (cm)**	**Dose (µGy)**	**LAC (cm^{-1})**	**MAC (cm^2/g)**	**HVL (cm)**
0.202	434.58	0.437	0.055	1.583	1.797	0.291	0.037	2.377
0.522	373.03	0.462	0.058	1.500	1.602	0.332	0.042	2.081
1.036	289.54	0.477	0.060	1.451	1.346	0.335	0.042	2.063
1.350	249.21	0.477	0.060	1.451	1.202	0.341	0.043	2.029

TABLE III. EXPERIMENTAL RESULTS FOR PB USING CS-137 AND CO-60

	Attenuation coefficients and HVL for lead slabs using Cs-137 gamma rays with initial dose of 474.76μGy.				**Attenuation coefficients and HVL for lead slabs using Co-60 gamma rays with initial dose of 1.906 μGy.**			
Thickness (cm)	**Dose (μGy)**	**LAC (cm^{-1})**	**MAC (cm^2/g)**	**HVL (cm)**	**Dose (μGy)**	**LAC (cm^{-1})**	**MAC (cm^2/g)**	**HVL (cm)**
0.154	400.46	1.105	0.097	0.627	1.744	0.576	0.050	1.211
0.472	274.69	1.159	0.102	0.597	1.428	0.611	0.053	1.132
0.812	190.42	1.125	0.099	0.615	1.169	0.602	0.053	1.151
0.966	164.63	1.096	0.096	0.632	1.079	0.589	0.051	1.176

TABLE IV. EXPERIMENTAL RESULTS FOR FE AND PB USING CS-137 LAC AND HVL FOR LEAD AND IRON SLABS USING CS-137 GAMMA RAYS WITH INITIAL DOSE OF 237.74μGY

Thickness (cm)	**Dose (μGy)**	**Experimental results**	
		LAC μ(cm^{-1})	**HVL (cm)**
0.356	182.72	0.7394	0.937
0.676	157.52	0.608	1.138
0.994	110.09	0.774	0.894
1.014	87.74	0.983	0.705
1.334	76.17	0.853	0.812
1.822	74.86	0.634	1.092
1.848	59.86	0.746	0.928
2.162	51.84	0.704	0.983

TABLE V. RESULTS OF FE BY PHY-X AND PY-MLBUF

Phy-X(Fe)							**Py-MLUBF (Fe)**				
Energy (MeV)	**Source**	**MAC (cm^2/g)**	**LAC (1/cm)**	**HVL (cm)**	**TVL (cm)**	**MFP (cm)**	**MAC (cm^2/g)**	**LAC (1/cm)**	**HVL (cm)**	**TVL (cm)**	**MFP (cm)**
6.62E-01	Cs (137)	0.073	0.578	1.199	3.982	1.729	7.35E-02	5.78E-01	1.1983	3.9806	1.730
8.00E-01		0.067	0.527	1.315	4.368	1.897	6.70E-02	5.27E-01	1.3147	4.3675	1.897
8.26E-01	Co (60)	0.066	0.519	1.336	4.437	1.927					
1.00E+00		0.060	0.472	1.469	4.881	2.120	6.00E-02	4.72E-01	1.4691	4.8804	2.118
1.17E+00	Co (60)	0.055	0.435	1.594	5.295	2.300	5.53E-02	4.35E-01	1.5927	5.2907	2.298
1.33E+00	Co (60)	0.052	0.408	1.701	5.650	2.454	5.18E-02	4.08E-01	1.7003	5.6482	2.450
1.50E+00		0.049	0.384	1.804	5.992	2.602	4.88E-02	3.84E-01	1.8037	5.9918	2.604
2.00E+00		0.043	0.336	2.065	6.861	2.980	4.27E-02	3.36E-01	2.0651	6.86	2.976

TABLE VI. RESULTS OF PB BY PHY-X AND PY-MLBUF

Phy-X(Pb)							**Py-MLUBF (Pb)**				
Energy (MeV)	**Source**	**MAC (cm^2/g)**	**LAC (1/cm)**	**HVL (cm)**	**TVL (cm)**	**MFP (cm)**	**MAC (cm^2/g)**	**LAC (1/cm)**	**HVL (cm)**	**TVL (cm)**	**MFP (cm)**
6.62E-01	Cs 137	1.10E-01	1.25E+00	0.5557	1.8459	0.800	1.10E-01	0.110	1.250	0.555	1.843
8.00E-01		8.87E-02	1.01E+00	0.6891	2.2892	0.990	8.87E-02	0.089	1.006	0.689	2.289
1.00E+00		7.10E-02	8.05E-01	0.8607	2.8591	1.2422	7.10E-02	0.071	0.805	0.861	2.859
1.17E+00	Co (60)	6.18E-02	7.01E-01	0.9891	3.2856	1.426	6.18E02	0.062	0.700	0.990	3.288
1.33E+00	Co (60)	5.61E-02	6.36E-01	1.0896	3.6194	1.572	5.61E-02	0.056	0.636	1.089	3.618
1.50E+00		5.22E-02	5.92E-01	1.1705	3.8884	1.689	5.22E-02	0.052	0.592	1.170	3.888
2.00E+00		4.61E-02	5.22E-01	1.3268	4.4074	1.915	4.61E-02	0.046	0.522	1.327	4.408

TABLE VII. RESULTS OF FE BY WINXCOM

WinXCOM (Fe)					
Photon energy (MeV)	**Scattering**		**Photoelectric absorption (cm^2/g)**	**Total attenuation**	
	Coherent (cm^2/g)	**Incoherent (cm^2/g)**		**With coherent scattering (cm^2/g)**	**Without coherent scattering (cm^2/g)**
6.620E-01	9.955E-04	7.159E-02	8.713E-04	7.346E-02	7.246E-02
8.000E-01	6.833E-04	6.575E-02	5.650E-04	6.699E-02	6.631E-02
1.000E+00	4.381E-04	5.916E-02	3.514E-04	5.995E-02	5.951E-02
1.022E+00	4.196E-04	5.853E-02	3.335E-04	5.928E-02	5.887E-02
1.173E+00	3.188E-04	5.466E-02	2.524E-04	5.526E-02	5.494E-02
1.250E+00	2.808E-04	5.292E-02	2.256E-04	5.350E-02	5.322E-02
1.332E+00	2.473E-04	5.122E-02	2.014E-04	5.181E-02	5.156E-02
1.500E+00	1.951E-04	4.811E-02	1.627E-04	4.883E-02	4.864E-02
2.000E+00	1.099E-04	4.107E-02	1.003E-04	4.265E-02	4.254E-02
2.000E+00	1.099E-04	4.107E-02	1.003E-04	4.265E-02	4.254E-02

TABLE VIII. RESULTS OF THE COMBINATION OF THE TWO SHIELDING MATERIALS

Fe+Pb combination, Py-MLUBF results							Fe+Pb combination, Phy-X results				
Energy (MeV)	**Source**	**MAC (cm^2/g)**	**LAC (1/cm)**	**HVL (cm)**	**TVL (cm)**	**MFP (cm)**	**MAC (cm^2/g)**	**LAC (1/cm)**	**HVL (cm)**	**TVL (cm)**	**MFP (cm)**
6.62E-01	**Cs(137)**	1.10E-01	1.25E+00	0.555	1.845	0.800	0.102	0.984	0.705	2.341	1.017
8.00E-01		8.87E-02	1.01E+00	0.689	2.289	0.990	0.084	0.808	0.858	2.851	1.238
1.00E+00		7.10E-02	8.05E-01	0.860	2.859	1.242	0.069	0.660	1.051	3.491	1.516
1.17E+00	**Co (60)**	6.18E-02	7.01E-01	0.989	3.285	1.426	0.060	0.580	1.195	3.971	1.724
1.33E+00	**Co (60)**	5.61E-02	6.36E-01	1.089	3.619	1.572	0.055	0.530	1.307	4.342	1.886
1.50E+00		5.22E-02	5.92E-01	1.170	3.8884	1.689	0.052	0.495	1.401	4.655	2.022
2.00E+00		4.61E-02	5.22E-01	1.326	4.407	1.915	0.045	0.435	1.592	5.287	2.296

TABLE IX. RESULTS OF THE COMBINATION OF THE TWO SHIELDING MATERIALS BY WINXCOM

WinXCOM (Pb+Fe)					
Photon energy (MeV)	**Scattering**		**Photoelectric absorption (cm^2/g)**	**Total attenuation**	
	Coherent (cm^2/g)	**Incoherent (cm^2/g)**		**With coherent scattering (cm^2/g)**	**Without coherent scattering (cm^2/g)**
6.620E-01	3.831E-03	6.586E-02	2.210E-02	9.180E-02	8.796E-02
8.000E-01	2.652E-03	6.056E-02	1.464E-02	7.785E-02	7.519E-02
1.000E+00	1.714E-03	5.454E-02	9.223E-03	6.548E-02	6.377E-02
1.022E+00	1.643E-03	5.399E-02	8.826E-03	6.445E-02	6.281E-02
1.173E+00	1.253E-03	5.044E-02	6.727E-03	5.851E-02	5.725E-02
1.250E+00	1.106E-03	4.884E-02	5.955E-03	5.613E-02	5.502E-02
1.332E+00	9.754E-04	4.728E-02	5.282E-03	5.398E-02	5.301E-02
1.500E+00	7.712E-04	4.443E-02	4.242E-03	5.053E-02	4.976E-02
2.000E+00	4.363E-04	3.795E-02	2.567E-03	4.436E-02	4.392E-02

Metals are commonly used in the design of radiation protection systems. Lead is dense and can be used against various high-energy applications of radiation. Lead possesses specific characteristics, e.g. its HVL increases with increase in energy [34]. To assess the shielding ability of a material, HVL is inversely related to the shielding effectiveness. With the increase in energy, HVL increases, due to the reducing intensity of incident gamma radiation to one half, more target thickness will be required. In iron, the HVL increases slightly. This is attributed to the small decrease in LAC with the decrease in iron content (Figures 1 and 2). We can see the significant differences in the HVL of Fe and Pb in Figures 1 and 3. The MAC of Fe and Pb can be seen in Figures 2 and 4. However, the combination is slightly changed in HVL and MAC. Gamma ray factor is larger through Cs-137 source and it is decreased in Co-60. The theoretical and experimental values of MAC, HVL, and TVL of gamma energy at 662, 1173 and 1333keV for lead and iron show that there is a good agreement between the theoretical and the experimental values [35].

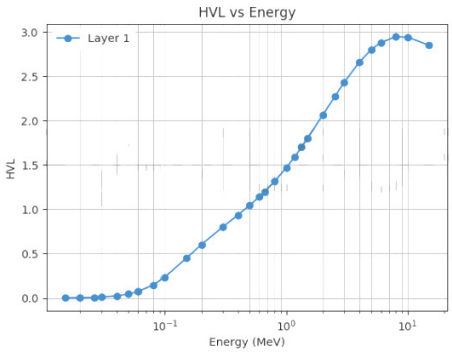

Fig. 1. Py-MLUBF (Fe) HVL vs energy.

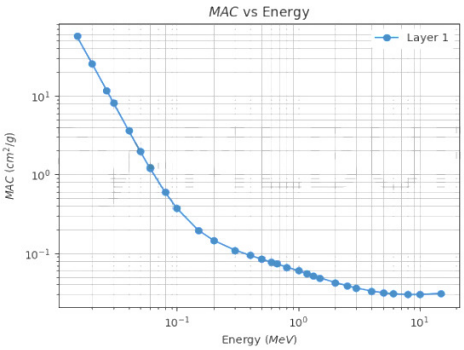

Fig. 2. Py-MLUBF (Fe) MAC vs energy.

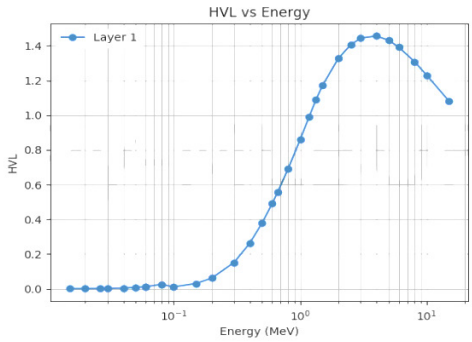

Fig. 3. Py-MLUBF (Pb) HVL vs energy.

IV. CONCLUSION

In this paper, mass attenuation coefficients and half-value layer values have been studied using COM, Phy-X, and Py-MLUBF. The codes provide quick calculations of gamma-ray

interaction parameters of the sample for the selected energies. The MAC values are found to reduce exponentially with increasing energy, whereas the HVL values are found to increase exponentially and radiation shielding values increase with increasing energy. The theoretical results are in good agreement with the results from the experimental work.

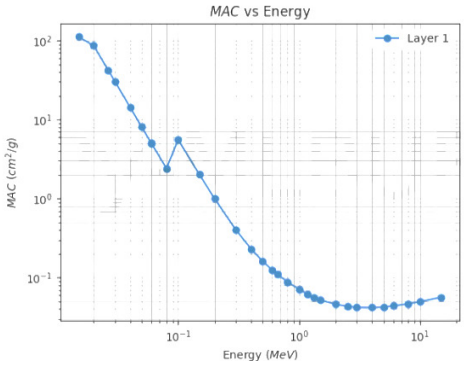

Fig. 4. Py-MLUBF (Pb) MAC vs energy.

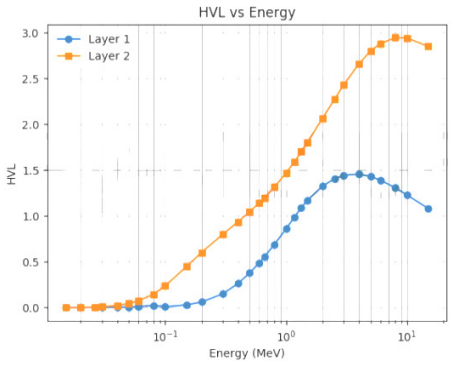

Fig. 5. Fe+Pb combination HVL vs energy.

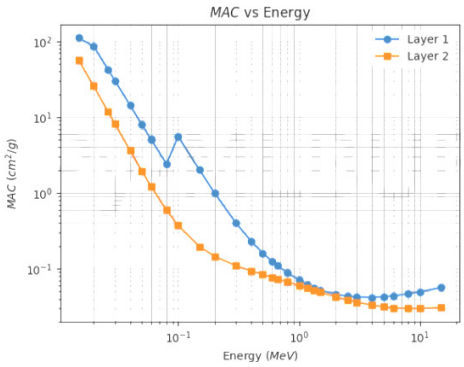

Fig. 6. Fe+Pb combination MAC vs energy.

The efficiency of the shielding material depends on its thickness and interaction energy. Knowing MAC, HVL, TVL, and MFP values may help determine which material reduces the radiation intensity more effectively. The results of this study may encourage the authorities to disseminate the radioprotection culture to the public. The heat and radiation resistance of materials such as Fe and Pb should be studied quantitatively in experiments and the results can help as a data base for future use. With this information at hand, future investigations will allow us to enhance radiation control.

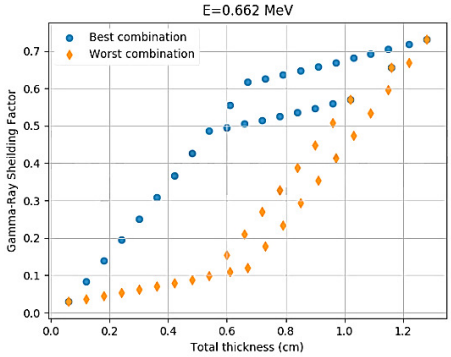

Fig. 7. Gamma Ray shielding factor for Fe+Pb calculated by Py-MLUBF for Cs-137.

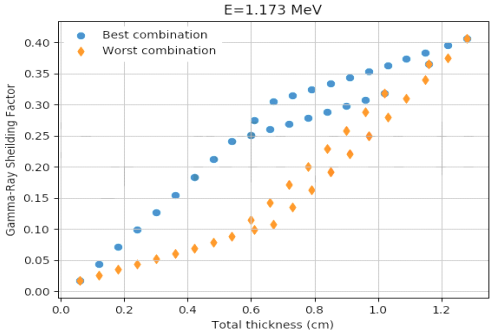

Fig. 8. Gamma Ray shielding factor for Fe+Pb calculated by Py-MLUBF for Co-60.

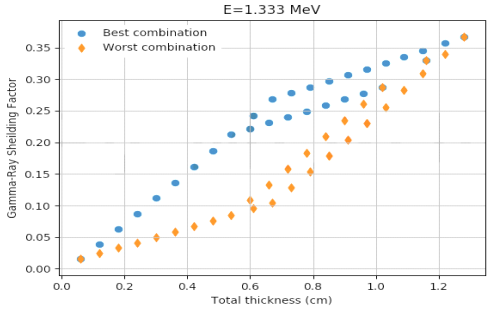

Fig. 9. Gamma Ray shielding factor for Fe+Pb calculated by Py-MLUBF for Co-60.

REFERENCES

[1] M. J. R. AL-Dhuhaibat, "Study of the shielding properties for some composite materials manufactured from polymer epoxy supported by cement, aluminum, iron and lead against gamma rays of the cobalt radioactive source (Co-60)," *International Journal of Application or Innovation in Engineering & Management*, vol. 4, no. 6, pp. 90–98, 2015.

[2] S. F. Olukotun *et al.*, "Investigation of gamma radiation shielding capability of two clay materials," *Nuclear Engineering and Technology*, vol. 50, no. 6, pp. 957–962, Aug. 2018, https://doi.org/10.1016/j.net.2018.05.003.

[3] S. Harb, A. H. El-Kamel, A. Abbady, A. M. Zahran, and F. A. Ahmed, "Natural Radioactivity Measurements of Basalt Rocks in Aden

governorate, South of Yemen on Gulf of Aden," *Journal of Applied Physics*, vol. 5, no. 6, pp. 39–48, Jan. 2014, https://doi.org/10.9790/4861-0563948.

[4] A. M. Abdelmonem, "Gamma rays and thermal neutron attenuation studies of special composite mixes for using in different applications," *Radiation Physics and Chemistry*, vol. 186, Sep. 2021, Art. no. 109541, https://doi.org/10.1016/j.radphyschem.2021.109541.

[5] Y. Elmahroug, B. Tellili, and C. Souga, "Determination of total mass attenuation coefficients, effective atomic numbers and electron densities for different shielding materials," *Annals of Nuclear Energy*, vol. 75, pp. 268–274, Jan. 2015, https://doi.org/10.1016/j.anucene.2014.08.015.

[6] U. S. Rajurkar and P. P. Pawar, "Measurement of attenuation coefficient and mean free path of some vitamins in the energy range 0.122-1.330 MeV," *Journal of Chemical and Pharmaceutical Research*, vol. 8, no. 5, pp. 852–856, 2016.

[7] N. Nakao *et al.*, "Attenuation length of high energy neutrons through a thick concrete shield measured by activation detectors at CHARM," *Journal of Nuclear Science and Technology*, vol. 57, no. 9, pp. 1022–1034, Sep. 2020, https://doi.org/10.1080/00223131.2020.1751740.

[8] N. Ibrahim, "Natural activities of 238U, 232Th and 40K in building materials," *Journal of Environmental Radioactivity*, vol. 43, no. 3, pp. 255–258, May 1999, https://doi.org/10.1016/S0265-931X(98)00033-2.

[9] E. Kavaz, N. Ekinci, H. O. Tekin, M. I. Sayyed, B. Aygun, and U. Perisanoglu, "Estimation of gamma radiation shielding qualification of newly developed glasses by using WinXCOM and MCNPX code," *Progress in Nuclear Energy*, vol. 115, pp. 12–20, Aug. 2019, https://doi.org/10.1016/j.pnucene.2019.03.029.

[10] M. B. Gili and F. Hila, "Investigation of Gamma-ray Shielding Features of Several Clay Materials Using the EPICS2017 Library," *Philippine Journal of Science*, vol. 150, pp. 1017–1026, Jul. 2021, https://doi.org/10.56899/150.05.13.

[11] A. M. Madbouly and A. El- Sawy, "Calculation of Gamma and Neutron Parameters for Some Concrete Materials as Radiation Shields for Nuclear Facilities," *International Journal of Emerging Trends in Engineering and Development*, vol. 8, no. 3, pp. 7–17, Aug. 2018, https://doi.org/10.26808/rs.ed.i8v4.02.

[12] H. Q. Vu, V. H. Tran, P. T. Nguyen, N. T. H. Le, and M. T. Le, "Radiation Shielding Properties Prediction of Barite used as Small Aggregate in Mortar," *Engineering, Technology & Applied Science Research*, vol. 10, no. 6, pp. 6469–6475, Dec. 2020, https://doi.org/10.48084/etasr.3880.

[13] F. A. Al-Mufadi, A. El-Taher, and G. A. Gamal, "Influence of γ-Irradiation on the Structural Properties of Indium Monoselenide Crystals," *Engineering, Technology & Applied Science Research*, vol. 6, no. 6, pp. 1264–1268, Dec. 2016, https://doi.org/10.48084/etasr.703.

[14] M. R. Abdullah, O. K. Alghazawi, and M. Al-Ayyad, "Non-uniform Heat Source and Radiation Effect on a Transient MHD Flow Past a Vertical Moving Plate with Inclined Magnetic Field and Periodic Heat Flux," *Engineering, Technology & Applied Science Research*, vol. 9, no. 4, pp. 4361–4366, Aug. 2019, https://doi.org/10.48084/etasr.2779.

[15] J. Räisänen, "Experimental arrangements for the simultaneous use of PIXE and complementary accelerator based techniques," *Nuclear Instruments and Methods in Physics Research Section B: Beam Interactions with Materials and Atoms*, vol. 49, no. 1, pp. 39–45, Apr. 1990, https://doi.org/10.1016/0168-583X(90)90213-E.

[16] M. I. Sayyed *et al.*, "Experimental and Theoretical Study of Radiation Shielding Features of CaO-K2O-Na2O-P2O5 Glass Systems," *Materials*, vol. 14, no. 14, Jan. 2021, Art. no. 3772, https://doi.org/10.3390/ma14143772.

[17] N. Singh, K. J. Singh, K. Singh, and H. Singh, "Gamma-ray attenuation studies of PbO–BaO–B2O3 glass system," *Radiation Measurements*, vol. 41, no. 1, pp. 84–88, Jan. 2006, https://doi.org/10.1016/j.radmeas.2004.09.009.

[18] E. O. Echeweozo, A. D. Asiegbu, and E. L. Efurumibe, "Investigation of kaolin - Granite composite bricks for gamma radiation shielding," *International Journal of Advanced Nuclear Reactor Design and Technology*, vol. 3, pp. 194–199, Jan. 2021, https://doi.org/10.1016/j.jandt.2021.09.007.

[19] K. Won-In, N. Sirikulrat, and P. Dararutana, "Radiation Shielding Lead-Free Glass Based on Barium-Bearing Glass Using Thailand Quartz Sands," *Advanced Materials Research*, vol. 214, pp. 207–211, 2011, https://doi.org/10.4028/www.scientific.net/AMR.214.207.

[20] O. Agar, "Investigation on Gamma Radiation Shielding Behaviour of CdO–WO3–TeO2 Glasses from 0.015 to 10 MeV," *Cumhuriyet Science Journal*, vol. 39, no. 33, pp. 983–990, 2018, https://doi.org/10.17776/csj.451770.

[21] N. R. Abd Elwahab, N. Helal, T. Mohamed, F. Shahin, and F. M. Ali, "New shielding composite paste for mixed fields of fast neutrons and gamma rays," *Materials Chemistry and Physics*, vol. 233, pp. 249–253, May 2019, https://doi.org/10.1016/j.matchemphys.2019.05.059.

[22] A. Martin, S. Harbison, K. Beach, and P. Cole, *An Introduction to Radiation Protection*, 7th Ed. Boca Raton, FL, USA: CRC Press, 2018.

[23] K. S. Mann, "Investigation of gamma-ray shielding by double layered enclosures," *Radiation Physics and Chemistry*, vol. 159, pp. 207–221, Jun. 2019, https://doi.org/10.1016/j.radphyschem.2019.03.007.

[24] K. S. Mann and S. S. Mann, "Py-MLBUF: Development of an online-platform for gamma-ray shielding calculations and investigations," *Annals of Nuclear Energy*, vol. 150, Jan. 2021, Art. no. 107845, https://doi.org/10.1016/j.anucene.2020.107845.

[25] L. Gerward, N. Guilbert, K. B. Jensen, and H. Levring, "WinXCom—a program for calculating X-ray attenuation coefficients," *Radiation Physics and Chemistry*, vol. 71, pp. 653–654, Oct. 2004, https://doi.org/10.1016/j.radphyschem.2004.04.040.

[26] M. I. Sayyed, M. Elsafi, A. H. Almuqrin, K. Cornish, and A. M. Elkhatib, "Novel Shielding Mortars for Radiation Source Transportation and Storage," *Sustainability*, vol. 14, no. 3, Jan. 2022, Art. no. 1248, https://doi.org/10.3390/su14031248.

[27] E. Sakar, O. F. Ozpolat, B. Alım, M. I. Sayyed, and M. Kurudirek, "Phy-X / PSD: Development of a user friendly online software for calculation of parameters relevant to radiation shielding and dosimetry," *Radiation Physics and Chemistry*, vol. 166, Jan. 2020, Art. no. 108496, https://doi.org/10.1016/j.radphyschem.2019.108496.

[28] M. S. Eid *et al.*, "Implementation of waste silicate glass into composition of ordinary cement for radiation shielding applications," *Nuclear Engineering and Technology*, vol. 54, no. 4, pp. 1456–1463, Apr. 2022, https://doi.org/10.1016/j.net.2021.10.007.

[29] A. El-Sayed Abdo, "Calculation of the cross-sections for fast neutrons and gamma-rays in concrete shields," *Annals of Nuclear Energy*, vol. 29, no. 16, pp. 1977–1988, Nov. 2002, https://doi.org/10.1016/S0306-4549(02)00019-1.

[30] G. ALMisned *et al.*, "Gamma-Ray Protection Properties of Bismuth-Silicate Glasses against Some Diagnostic Nuclear Medicine Radioisotopes: A Comprehensive Study," *Materials*, vol. 14, no. 21, Jan. 2021, Art. no. 6668, https://doi.org/10.3390/ma14216668.

[31] A. H. Almuqrin and M. I. Sayyed, "Gamma Ray Shielding Properties of Yb3+-Doped Calcium Borotellurite Glasses," *Applied Sciences*, vol. 11, no. 12, Jan. 2021, Art. no. 5697, https://doi.org/10.3390/app11125697.

[32] M. I. Sayyed, "Half value layer, mean free path and exposure buildup factor for tellurite glasses with different oxide compositions," *Journal of Alloys and Compounds*, vol. 695, pp. 3191–3197, Feb. 2017, https://doi.org/10.1016/j.jallcom.2016.11.318.

[33] F. Akman, O. Agar, M. R. Kacal, and M. I. Sayyed, "Comparison of experimental and theoretical radiation shielding parameters of several environmentally friendly materials," *Nuclear Science and Techniques*, vol. 30, no. 7, Jun. 2019, Art. no. 110, https://doi.org/10.1007/s41365-019-0631-1.

[34] R. Singh, S. Singh, G. Singh, and K. S. Thind, "Gamma Radiation Shielding Properties of Steel and Iron Slags," *New Journal of Glass and Ceramics*, vol. 7, no. 1, 2017, Art. no. 72939, https://doi.org/10.4236/njgc.2017.71001.

[35] A. B. Aziz, Md. F. Rahman, and M. M. Prodhan, "Comparison of Lead, Copper and Aluminium as Gamma Radiation Shielding Material through Experimental Measurements and Simulation Using MCNP Version 4c," *International Journal of Contemporary Research and Review*, vol. 9, no. 8, pp. 20193–20206, Aug. 2018, https://doi.org/10.15520/ijcrr/2018/9/08/584.